sciendo

Mathematical Modelling in Civil Engineering
Vol. 16-No. 4 : 13-24-2021
Doi: 10.2478/mcee-2021-0017

SIMULATION OF SPATIALLY VARIABLE ARTIFICIAL EARTHQUAKE: A CASE STUDY OF DIFFERENT SITE CONDITIONS

Rachid DERBAL - PhD, Department of Civil Engineering, University of Ain Temouchent, Algeria / RISk Assesment & Management Laboratory (RISAM), University of Tlemcen, Algeria, e-mail: rachid.derbal@univ-temouchent.edu.dz

Nassima BENMANSOUR - PhD, RISk Assesment & Management Laboratory (RISAM), University of Tlemcen, Algeria/ e-mail: nassima.benmansour@univ-tlemcen.dz

Mustapha DJAFOUR – Lecturer, PhD, RISk Assesment & Management Laboratory (RISAM), University of Tlemcen, Algeria, e-mail: mustapha.djafour@univ-tlemcen.dz

Abstract: The dynamic analysis of structures under seismic ground motions is a major issue in earthquake engineering. The seismic ground motions observed at the surface are variables in space and time. The main causes of this variability come from seismic waves propagation between the source and the site, and in particular the local geological site conditions. For this purpose, it is essential to consider all these factors of the spatial variability of seismic ground motion when representing seismic loading to be applied to any structure. Given the scarcity of real seismic records, many researchers suggest the use of artificial or synthetic seismic motions. The main objective of this study is the simulation of spatially variable artificial seismic motions by considering all fact of factors of the seismic spatial variability, especially site local conditions. In this sense, a simulation technique of spatially variable seismic motions is developed using the spectral representation method. By adopting the unconditional simulation approach, the target seismic motion in bedrock is defined by the Clough-Penzien spectral model and a specified coherency loss model. Then, the simulated ground motions in the bedrock are projected on the surface by considering amplification site effect. The results showed that the simulated artificial seismic motions are strongly conditioned by the local site conditions.

Keywords: Spatial variability – coherency loss – local site conditions – site amplification – simulation technique – artificial seismic motions.

1. Introduction

It is commonly accepted that extended structures are the most affected by the spatial variability of seismic ground motion. Indeed, this spatial variability result from several factors, mainly, the effect of coherency loss of seismic waves, the wave passage effect and the local site effect [1,2].

The rarity of seismic events as well as other considerations have led to the installation of several networks of accelerographs on given sites, such as the network of El Centro in the USA, SMART1 and LSST in Lotung, Taiwan and EURO-SEISTEST in Greece. Knowledge of the probabilistic characteristics of earthquakes has been significantly improved thanks to analysis of recording data of these networks of accelerographs [3,4].

Because recordings of closely spaced earthquake ground motions are very rare, response analysis of extended structures requires simulation of artificial ground motions by adopting a specified spatial variability model [2].

In the literature, several studies on the effect of spatial variability of seismic ground motion on extended structures have been carried out. A large number of these studies consider that the site, where the structure is implanted, is uniform and homogeneous, i.e. that only the effects of coherency loss and wave passage, due to the propagation of seismic waves, are adopted. Most of these studies have led to empirical or analytical models [1,5–10].

However, for a site composed by various types of soil at different locations, the seismic wave propagation and frequency content are affected. Consequently, the intensity of earthquakes is directly related to the parameters of foundation soil. Therefore, this assumption of uniform site gives rise to an inaccurate representation of the adopted seismic ground motion [11–16].

It should be noted that during the Michoacán earthquake in 1985 of magnitude equal to 8.2 on Richter scale, the most significant damage was observed in Mexico City, yet located about 400 km from the epicenter. This is mainly due to the location of this city on a sedimentary basin, which has led to a dispersion of the seismic waves and consequently to an amplification of the oscillations. In fact, the amplification effect of seismic waves can be very significant in the case of sites composed of sedimentary deposits [17].

This phenomenon of the local site effect has encouraged several researchers to undertake studies on the influence of this effect on the estimation of seismic ground motions [2,12,13,18–21]. Further research has addressed the assessment of the impact of the local site effect on dynamic response of extended structures [11,22,23].

In recent years, studies on the spatial variability of seismic ground motion considering the site effect have been undertaken. In the beginning, the site effect was incorporated into the definition of spatial ground motion by simple approaches or simplified models. Next, researchers started to study this phenomenon by adopting more realistic models [10,16,19,20,24]. Indeed, the analysis of the site response can be very complex, especially if a site has very divergent characteristics. It should be noted that sedimentary deposits can generate a high amplification under seismic excitations. Recent research of the influence of spatial variability of seismic ground motion has led to generation methods of artificial or synthetic spatially variable seismic motions [2,11,19,25–30].

It should be noted that the numerical and statistical processing of the available recordings posed many theoretical and practical difficulties given the highly non-stationary nature of earthquakes, as well as the relative lack of available data. The models established are related to the methodology adopted by the data analysis, which explains, for example, the limited domain of validity of a given model. Hence, the great need to simulate artificial seismic ground motions useful for the dynamic analysis of extended structures [2,12,31,32].

The main objective of this study is to simulate artificial seismic ground motions on surface. A detailed simulation technique of spatially variable seismic ground motions is presented. A case study is presented to validate the developed simulation technique.

2. Description of spatially variable seismic ground motions

2.1 Coherency loss effect

The coherency loss effect includes the influence of the multiples diffractions, reflections, interferences on the seismic wave propagating from the source to the site. The coherency loss effect is defined in the frequency domain by [1,11]:

$$\gamma_{a,b}(\omega) = \left|\gamma_{a,b}(\omega)\right| exp\left(-i\frac{\omega d_{a,b}}{V}\right) \quad (1)$$

Where :

ω is the angular frequency.

$d_{a,b}$ is the projected horizontal distance along the direction of wave propagation (from point a to point b).

V is the apparent speed of the waves.

Wave passage effect

The wave passage effect is directly related to the differences in the arrival times of the seismic wave at different stations. It is purely deterministic when the phase of the seismic signal is perfectly known. The wave passage effect is introduced by applying a time shift which is equal to [1,11]:

$$D_T = d_{a,b}/V \quad (2)$$

2.2 Local site effect

The local site effect is related to the local variability of the soil profile on site. For the point *a* located in bedrock having the vertical projection on the surface at point *a*', the transfer function for the shear wave propagation in a horizontal layer of soil is given by [33,34] :

$$H_{a'}(i\omega) = \frac{U_{a'}(i\omega)}{U_a(i\omega)} = \frac{(1+r_{a'}-i\xi_{a'})exp(-i\omega\tau_{a'}(1-2i\xi_{a'}))}{1+(r_{a'}-i\xi_{a'})exp(-2i\omega\tau_{a'}(1-2i\xi_{a'}))} \quad (3)$$

With :

$\xi_{a'}$ is the damping coefficient calculated from the energy dissipation due to the propagation of seismic waves.

$\tau_{a'}$ is the propagation time of the wave from point *a* to *a'* and $r_{a'}$ is the reflection coefficient.

3. Simulation Technique of spatially variable seismic ground motions

Considering a vector of one-dimensional multi-variable stationary stochastic processes consisting of the components process $g_k(t)$; *k = 1,2, ..., n.* and zero means such that [2,35] :

$$E[g_k(t)] = 0; (k = 1,2, \dots, n) \quad (4)$$

The cross correlation matrix is given by [35]:

$$R(\tau) = \begin{bmatrix} R_{11}(\tau) & R_{12}(\tau) & \dots\dots & R_{1n}(\tau) \\ R_{21}(\tau) & R_{22}(\tau) & \dots\dots & R_{2n}(\tau) \\ \dots\dots & \dots\dots & \dots\dots & \dots\dots \\ R_{n1}(\tau) & R_{n2}(\tau) & \dots\dots & R_{nn}(\tau) \end{bmatrix} \quad (5)$$

The corresponding cross power spectral density matrix is [2,35] :

$$S(i\omega) = \begin{bmatrix} S_{11}(\omega) & S_{12}(i\omega) & \dots\dots & S_{1n}(i\omega) \\ S_{21}(i\omega) & S_{22}(\omega) & \dots\dots & S_{2n}(i\omega) \\ \dots\dots & \dots\dots & \dots\dots & \dots\dots \\ S_{n1}(i\omega) & S_{n2}(i\omega) & \dots\dots & S_{nn}(\omega) \end{bmatrix} \quad (6)$$

Using the coherency loss function (Eq. 1), the cross power spectral density matrix at the bedrock becomes [1,11,35]:

$$S_{a,b}(\omega) = \left[\sqrt{S_a(\omega)\, S_b(\omega)}\, \gamma_{a,b}(\omega)\right] \quad a, b = 1,2, \dots, n. \quad (7)$$

Then, the cross power spectral density matrix at the surface level is calculated as follows [11,33,36]:

$$S_{a'}(\omega) = |H_{a'}(i\omega)|^{\,2} S_g(\omega) \quad a' = 1,2, \dots, n. \quad (8)$$

$$S_{a',b'}(\omega) \quad = H_{a'}(i\omega) H^*_{b'}(i\omega) S_{a',b'}(i\omega) \quad a' \neq b' \quad (9)$$

The subscript "*" represents the complex conjugate.

The cross power spectral density matrix at the surface is decomposed using the Cholesky decomposition method [2,4,11,35] :

$$S_{a',b'}(\omega) = L(\omega) L^{T*}(\omega) \quad (10)$$

Using the real and polar elements of the matrix $L(\omega)$, the stationary stochastic processes $g_k(t)$ are simulated by the following series when $N \to \infty$ [31,32]:

$$g_k(t) = 2\sum_{m=1}^{n}\sum_{l=1}^{N}|L_{km}(\omega)|\sqrt{\Delta\omega}\,cos(\omega_l - \theta_{km}(\omega_l) + \phi_{ml}) \quad (11)$$

With :

$$\omega_l = l\Delta\omega \text{ and } \Delta\omega = \omega_u/N \quad (12,13)$$

Knowing that N is the number of angular frequency steps to reach the cutoff frequency ω_u.

The non-stationarity of seismic motions is incorporated using the Jennings modulation function [37] :

$$\zeta(t) = \begin{cases} (t/t_0)^2 & 0 \le t \le t_0 \\ 1 & t_0 < t \le t_n \\ exp[-\alpha(t-t_n)] & t_n < t \le T \end{cases} \quad (14)$$

With : t_0 = 2 s, t_n= 10 s and α = 0.155 [37].

Finally, the artificially simulated seismic movements will have the following form [11–13,19]:

$$f_j(t) = \zeta(t)\cdot g_k(t), \quad k = 1,2,\dots,n. \quad (15)$$

4. Target seismic ground motion at the bedrock

The seismic motion in the bedrock is defined by the Clough-Penzien spectral model [1,11,35]:

$$S_g(\omega) = |H_P(\omega)|^2 S_0(\omega) \quad (16)$$

The first term of the equation (16) is $|H_P(\omega)|^2$ defined by the Clough-Penzien high pass filter and it is given by the following form [38]:

$$|H_P(\omega)|^2 = \frac{\omega^4}{\left(\omega_f^2-\omega^2\right)^2+\left(2\omega_f\omega\xi_f\right)^2} \quad (17)$$

Where ω_f and ξ_f are the central frequency and the damping rate of the high pass filter.

While, the second term of the equation (14) is $S_0(\omega)$ defined by the Kanai-Tajimi power spectral density function [39].

Where ω_g and ξ_g are the central frequency and the damping rate of the Kanai-Tajimi power spectral density. Γ is a scaling factor as a function of the intensity of the seismic ground motion [11,19,35,39].

$$S_0(\omega) = \frac{\omega_g^4+4\xi_g^2\omega_g^2\omega^2}{\left(\omega_g^2-\omega^2\right)^2+4\xi_g^2\omega_g^2\omega^2}\Gamma \quad (18)$$

So formula 14 becomes :

$$S_g(\omega) = \frac{\omega^4}{\left(\omega_f^2-\omega^2\right)^2+\left(2\omega_f\omega\xi_f\right)^2}\cdot\frac{\omega_g^4+4\xi_g^2\omega_g^2\omega^2}{\left(\omega_g^2-\omega^2\right)^2+4\xi_g^2\omega_g^2\omega^2}\Gamma \quad (19)$$

5. Numerical example

The scheme illustrated in Fig. 1 represents a bridge frame composed of three piers distant by 200 m. The contact of these piers with the surface of soil are a', b' and c'. Their vertical projections on the bedrock are a, b and c respectively (Fig. 1). In this study, the sites parameters are chosen on the basis site classification described by RPOA 2008 (Algerian seismic code for bridges) [40]. The site classes adopted are S2, S3 and S4 corresponding to B, C and D ground types in the Eurocode 8 [41], respectively. The parameters of the bedrock and the selected sites are given in Table 1.

Table 1

Parameters of adopted sites [40]

Site 1 (S3)				*Site 2 (S2)*				*Site 3 (S4)*				*Bedrock*		
ρ_1 *(KN/m³)*	v_1 *(m/s)*	ξ_1	h_1 *(m)*	ρ_2 *(KN/m³)*	v_2 *(m/s)*	ξ_2	h_2 *(m)*	ρ_3 *(KN/m³)*	v_3 *(m/s)*	ξ_3	h_3 *(m)*	ρ_{sub} *(KN/m³)*	v_{sub} *(m/s)*	ξ_{sub}
16	300	5%	25	20	450	5%	15	15	150	5%	35	25	965	5%

Table 2 describes the parameters of the Clough-Penzien spectral model with a maximum acceleration of 0.2 g and a target signal duration of 40 s [19,42]. This spectral density model is illustrated in Fig. 2.

Table 2

Parameters of the Clough-Penzien spectral model (Bi & Hao, 2012; Li, Hao, Li, Bi, & Chen, 2017)

ω_g (Hz)	ξ_g	ω_f (Hz)	ξ_f	Γ (m^2/s^3)
10π	0.6	0.5π	0.6	0.0031

The selected coherency loss model to describe the seismic ground motion between the points located at the bedrock is Harichandran and Vanmarcke model [10]. It is given by the following equation :

$$\gamma_{a,b}(\omega, d_{a,b}) = A \cdot \exp\left(-\frac{2(1-A+\alpha A)|d_{a,b}|}{\alpha\Theta(\omega)}\right) + (1-A) \cdot \exp\left(-\frac{2(1-A+\alpha A)|d_{a,b}|}{\alpha\Theta(\omega)}\right) \quad (20)$$

With: $$\Theta(\omega) = \mathrm{k}\left[1 + \left(\frac{c}{2\pi\omega_0}\right)\right] \quad (21)$$

Where : *A, α, k,* ω_0 and *b* are constants. These values are given in Table 3 [10].

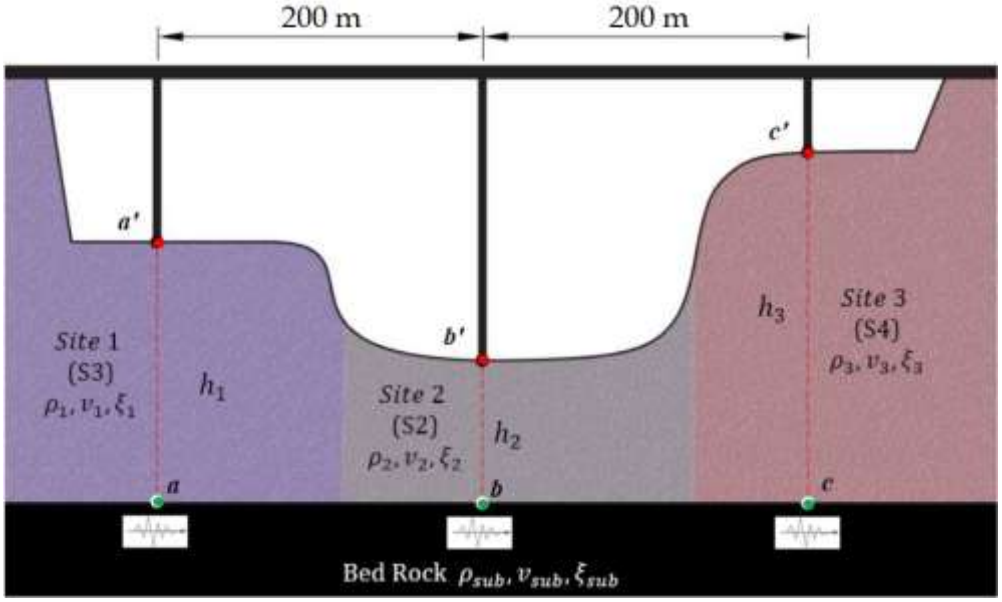


Fig. 1 - Bridge frame installed at different sites

Table 3

Parameters of the Harichandran and Vanmarcke coherency loss model [10]

A	α	k (m)	ω_0 (rad/s)	b
0.626	0.022	19700	1.109×10^{-3}	3.47

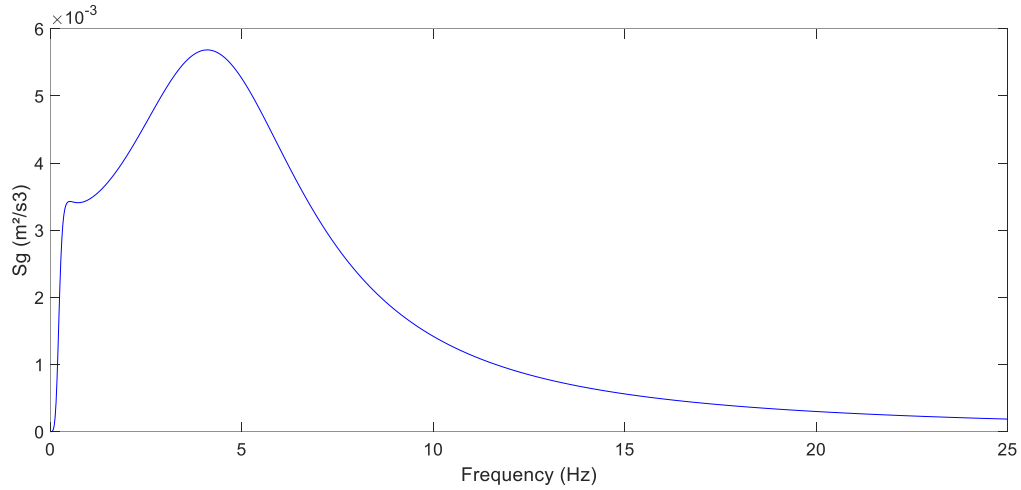


Fig. 2 - Clough-Penzien spectral density model

5.1 Cases of simulation of artificial seismic movements

Using the simulation technique described above, artificial seismic ground motions were simulated in acceleration, velocity and displacement. Three simulation cases are considered:

- Case 01: is the uniform case i.e. that the spatial variability of the seismic motion is neglected.
- Case 02: is the case where the spatial variability of the seismic motion is defined only by coherency loss and wave passage effects i.e. that the local site effect is neglected.
- Case 03: is the case where all the factors of the spatial variability of seismic ground motion are considered (coherency loss, wave passage and local site effects).

5.2 Simulation of ground motions by neglecting the seismic spatial variability

The first step is to simulate the artificial seismic motions at the bedrock in the uniform case i.e. by neglecting the seismic spatial variability. This is used for the reproduction and verification of the target seismic ground motion.

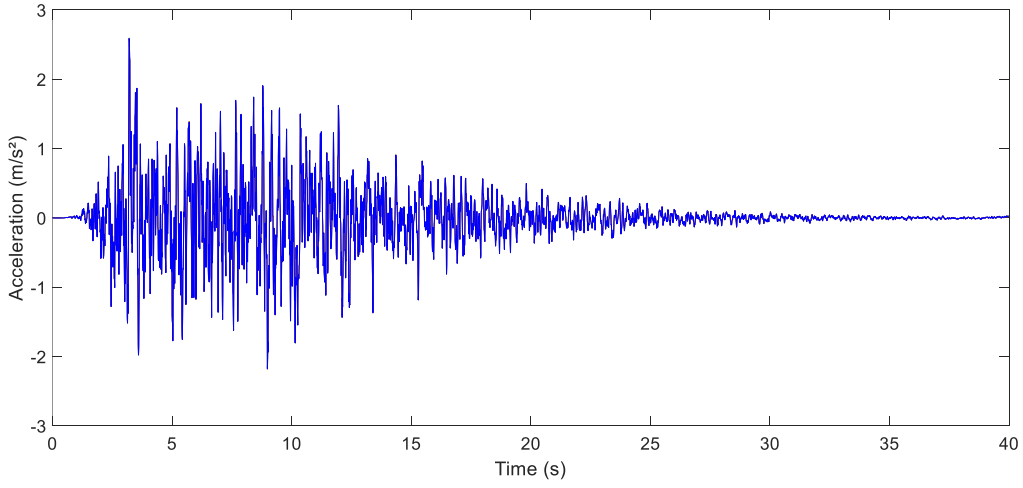


Fig. 3 - Simulated accelerations by neglecting the seismic spatial variability

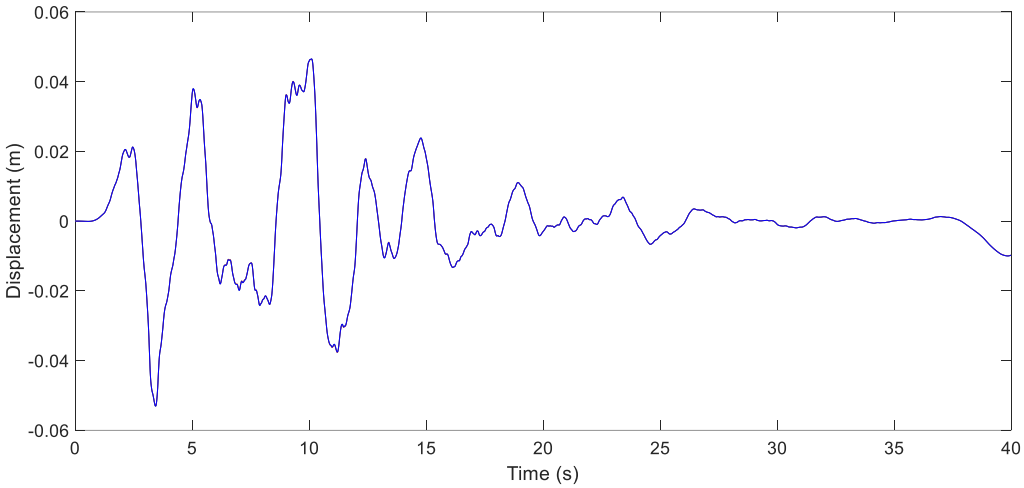


Fig. 4 - Simulated displacements by neglecting the seismic spatial variability

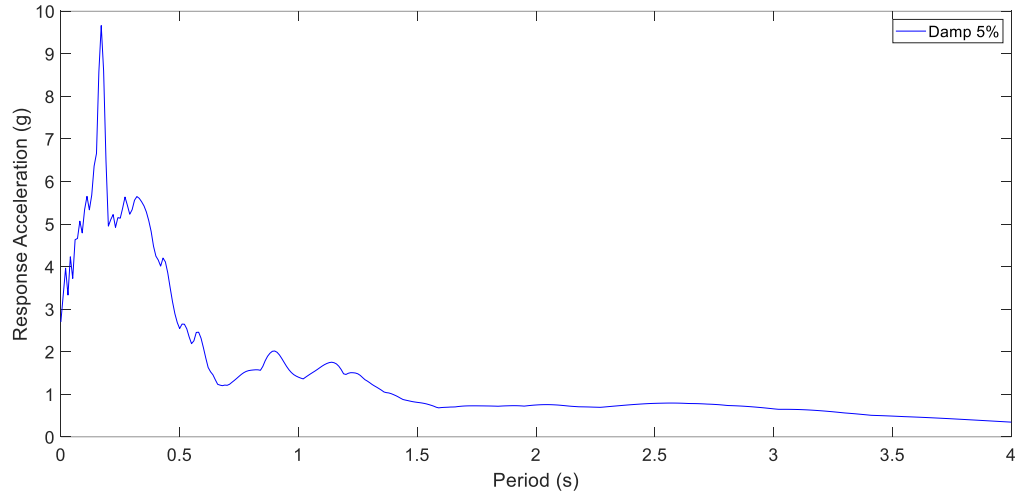


Fig. 5 - Response spectrum of simulated accelerations by neglecting the seismic spatial variability

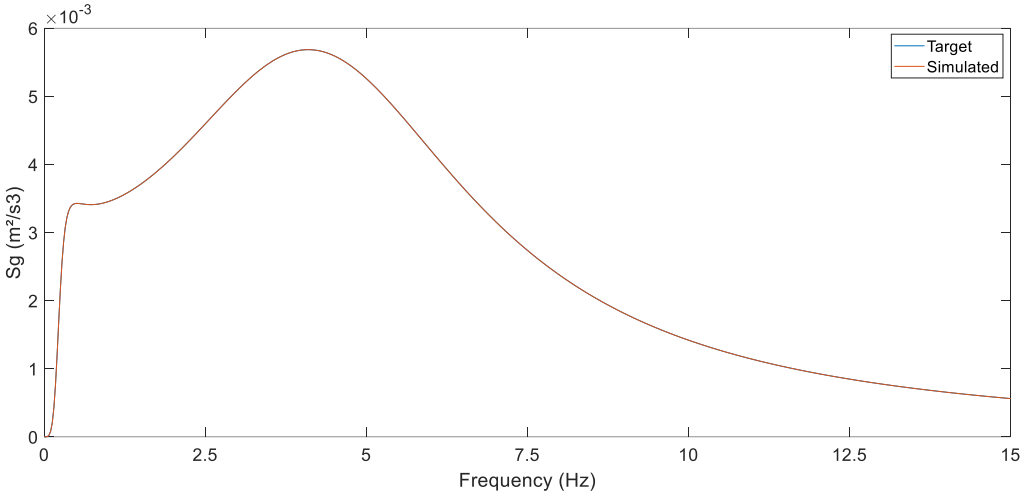


Fig. 6 - Comparison of power spectral densities by neglecting the seismic spatial variability

The simulated artificial seismic motions are illustrated in figures 3 to 4. It is observed that the simulated motions are perfectly identical and have the following characteristics: maximum acceleration: PGA = 0.26 g ; maximum velocity: PGV = 0.22 cm/s ; maximum displacement: PGD = 0.053 m.

Adopting a damping of 5%, the response spectrum of the simulated motions is shown in Fig. 6. The comparison of the power spectral densities of the simulated seismic motions and the target spectral density model gives a perfect match (Fig. 6).

5.3 Simulation of spatially variable seismic motions (coherency loss and waves passage effects)

The results of the second simulation case (coherency loss and wave passage effects) are illustrated in figures 7 and 8. The simulated artificial accelerations have a PGA of 0.26 g, 0.23 g and 0.24 g at the points *a*, *b* and *c* respectively. The maximum displacements (PGD) recorded are 0.053 m, 0.047 m and 0.048 m. We observe that the simulated seismic motions in this second case and those of the uniform case are very close. The response spectrum of the simulated seismic motions, shown in Fig. 9, have almost the same frequency content.

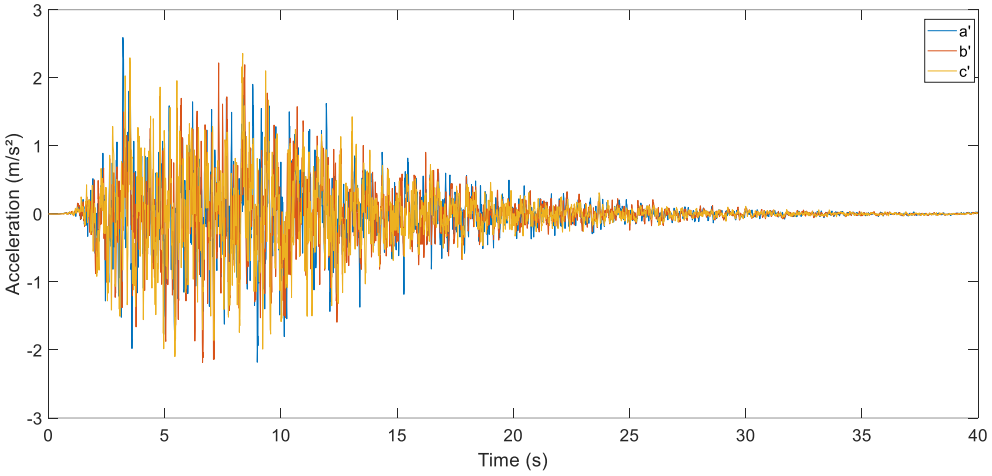


Fig. 7 - Simulated spatial variable accelerations (coherency loss and waves passage effects)

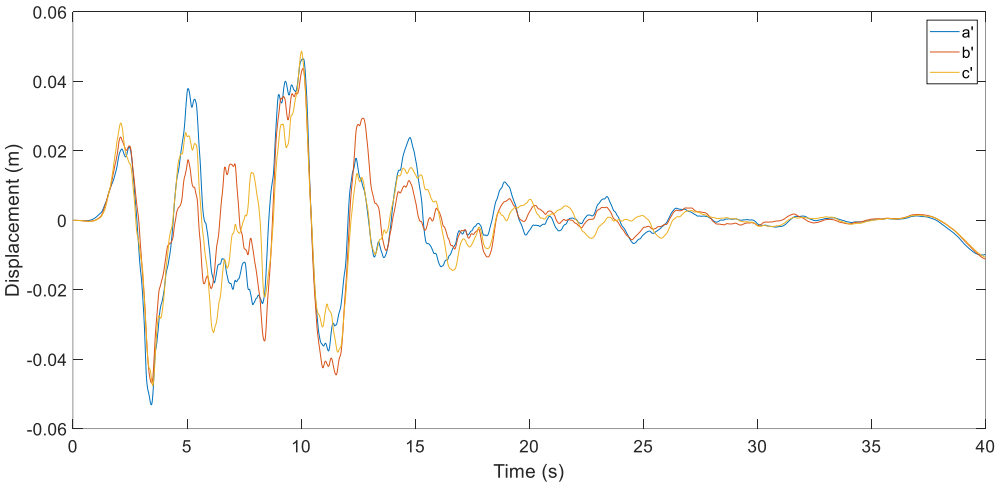


Fig. 8 - Simulated spatial variable displacements (coherency loss and waves passage effects)

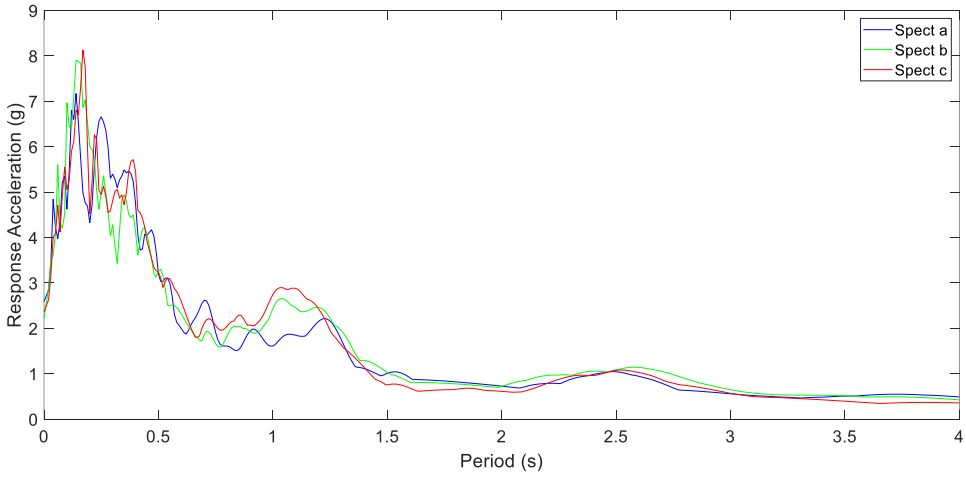


Fig. 9 - Response spectrum of spatial variable accelerations (coherency loss and waves passage effects)

5.4 Simulation of spatially variable seismic motions (coherency loss, wave passage and local site effects)

In this part, the simulated artificial seismic motions at the bedrock are projected at the surface by site amplification. For this, the transfer functions at the points located on the surface a', b' and c' are calculated and illustrated in Fig. 10. The maximum amplification is measured for a soft soil at point c' and it is equal to 3.92 corresponding to a predominant frequency of 1.02 Hz. While the lowest amplification is measured for a firm ground at point b' with a value of 1.8 corresponding to a predominant frequency of 6.85 Hz (Fig. 10).

Figures 11 and 12 give the simulated artificial accelerations, velocities and displacements in the third case, where all factors of seismic variability are considered, namely the coherence loss, wave passage and local site effects.

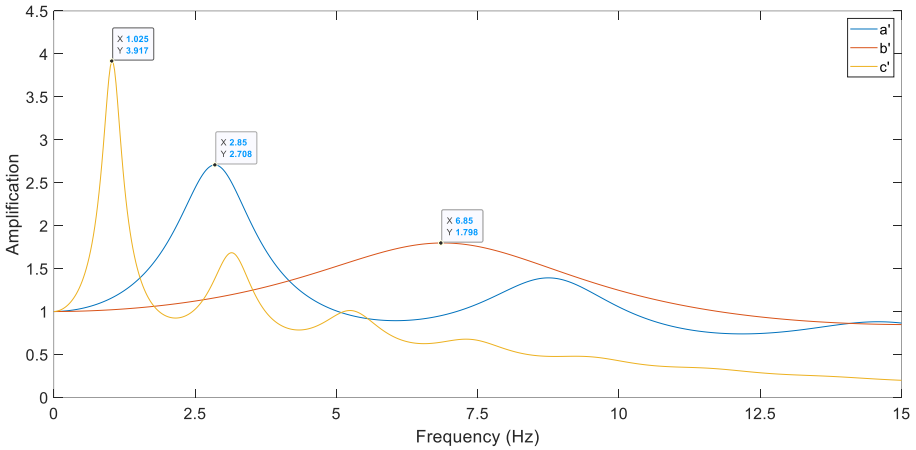


Fig. 10 - Transfer functions at the surface of sites

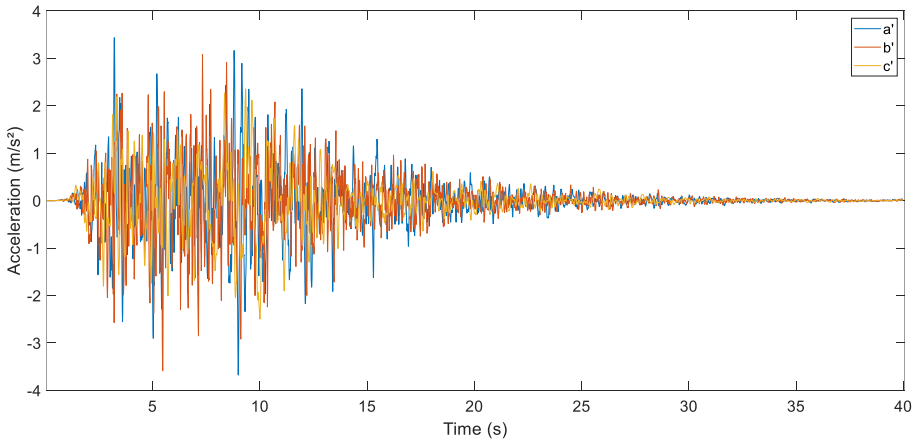


Fig. 11 - Simulated accelerations in the case considering all factors of seismic variability

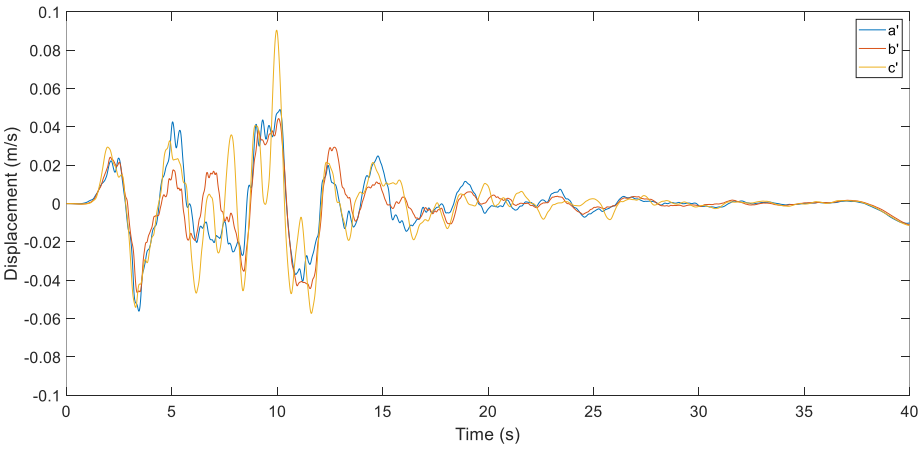


Fig. 12 - Simulated displacements in the case considering all factors of seismic variability

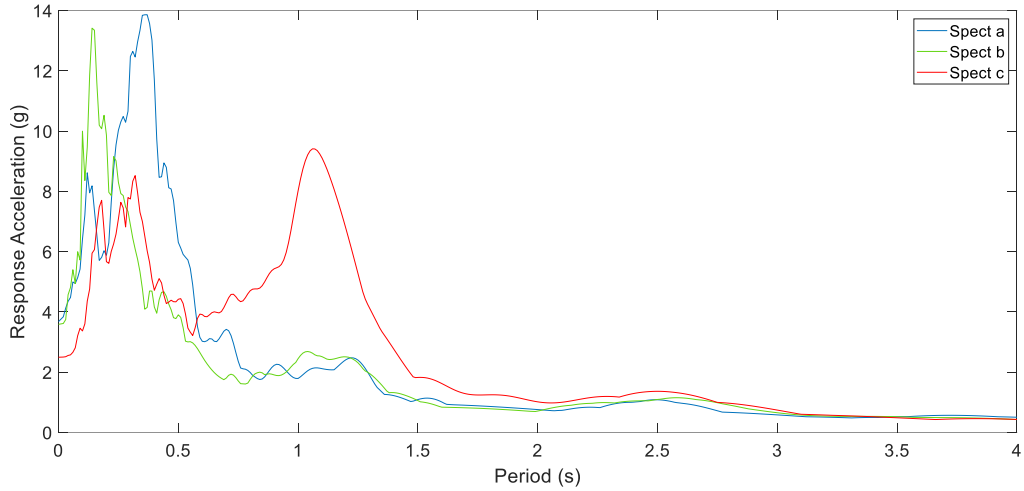


Fig. 13 - Response spectrum of simulated accelerations in the case considering all factors of seismic variability

The simulated accelerations have a PGA of 0.38 g, 0.37 g and 0.25 g at points *a'*, *b'* and *c'* respectively. The maximum displacements (PGD) measured are 0.056 m, 0.047 m and 0.091 m. We observe that the simulated seismic ground motions are greater than those resulting from the uniform case and the second case (coherency loss and wave passage). The Fig. 13 illustrates the response spectrum of the simulated artificial accelerations. The difference in the frequency content is very pronounced, especially for the soft site at the point *c'*.

Table 4

PGA and PGD values of the different simulation cases

	PGA (g)			*PGD (m)*		
Cases ~~*Points*~~	*a'*	*b'*	*c'*	*a'*	*b'*	*c'*
Case 01	0.26	0.26	0.26	0.053	0.053	0.053
Case 02	0.26	0.23	0.24	0.053	0.047	0.046
Case 03	0.38	0.37	0.25	0.056	0.047	0.091

A summary of the PGA and PGD values of the different simulation cases is given in Table 4. Comparing the results of the three simulation cases, we observe that the case taking into account all the factors of seismic variability gives maximum accelerations of 0.38 g for a firm site. This is probably due to a closeness of the frequencies of the firm site and the target seismic motion.

The maximum displacement is also recorded at the third simulation case for the soft site.

6. Conclusions

The work carried out consists to the simulation of artificial seismic ground motions considering all factors of the seismic spatial variability. A simulation technique of artificial seismic ground motions is developed. A case study is presented to validate this simulation technique and to evaluate the influence of the variation of site conditions on the simulated seismic ground motions.

Adopting three cases of simulations, the artificial seismic motions were simulated in acceleration and displacement. The uniform seismic motion simulation case is used for a reproduction and verification of the target seismic ground motion.

The results of these simulations demonstrate that the simulated artificial seismic motions of the first case (neglecting the seismic spatial variability) and the second case (spatially variable with considering only coherency loss and wave passage effects) are very similar. In addition, the frequency content is not influenced by these simulation cases. Therefore, characterizing a spatially variable seismic motion by a coherency loss model and the wave passage effect is not enough.

Therefore, seismic analysis of extended structures using this consideration will give the same results as the classical methods, that which considers a uniform seismic motion.

The simulation case where all factors of seismic spatial variability are considered gives the highest simulated artificial seismic motions. It is clearly shown that the local site effect has an important influence on the seismic ground motion. Where, the site amplification is related to the characteristics of soil foundation. This amplification can greatly modify the intensity and the frequency content of seismic ground motions.

References

[1] Der Kiureghian, A. (1996). A coherency model for spatially varying ground motions. *Earthquake Engineering and Structural Dynamics*, 25(1), 99–111. DOI: 10.1002/(sici)1096-9845(199601)25:1<99::aid-eqe540>3.3.co;2-3.

[2] Konakli, K. & Der Kiureghian A. (2012). Simulation of spatially varying ground motions including incoherence, wave-passage and differential site-response effects. *Earthquake Engineering & Structural Dynamics*,41(3), 495–513. DOI: 10.1002/eqe.1141.

[3] Harichandran, RS. (1999). *Spatial Variation of Earthquake Ground Motion - What is it , how do we model it , and what are its engineering implications ?*, Manuscript corresponding to seminars presented at University of Puerto Rico.

[4] Zerva, A. *Spatial variation of seismic ground motions: modeling and engineering applications*. CRC Press. DOI: 10.1201/9781420009910.

[5] Abrahamson, N. (2008). Ground Motion Models. *Geotechnical Earthquake Engineering and Soil Dynamics IV, Reston, VA: American Society of Civil Engineers*. DOI: 10.1061/40975(318)2.

[6] Zendagui, D. Berrah, MK. & Kausel E. (1999). Stochastic deamplification of spatially varying seismic motions. *Soil Dynamics and Earthquake Engineering*, 18(6), 409–421. DOI: 10.1016/S0267-7261(99)00015-9.

[7] Zendagui, D. & Berrah MK. (2002). Spatial variation of seismic motion induced by propagation of body waves. *Soil Dynamics and Earthquake Engineering*, 22(9–12), 805–811. DOI: 10.1016/S0267-7261(02)00102-1.

[8] Zerva, A. & Shinozuka M. (1991). Stochastic differential ground motion. *Structural Safety*, 10(1–3), 129–143. DOI: 10.1016/0167-4730(91)90010-7.

[9] Zerva, A. (1992). Seismic loads predicted by spatial variability models. *Structural Safety*, 11(3–4), 227–243. DOI: 10.1016/0167-4730(92)90016-G.

[10] Harichandran, RS. & Vanmarcke EH. (1986). Stochastic variation of earthquake ground motion in space and time. *Journal of Engineering Mechanics*, 112(2), 154–174. DOI: 10.1061/(asce)0733-9399(1986)112:2(154).

[11] Bi, K. Hao H. & Ren W. (2010). Response of a frame structure on a canyon site to spatially varying ground motions. *Structural Engineering and Mechanics*, 36(1), 111–127. DOI: 10.12989/sem.2010.36.1.111.

[12] Derbal, R. Benmansour, N. Djafour, M. Matallah M. & Ivorra S. (2019). Viaduct seismic response under spatial variable ground motion considering site conditions. *Earthquake and Structures*, 17(6), 557–566. DOI: 10.12989/eas.2019.17.6.557.

[13] Derbal, R. Benmansour, N. Djafour, M. Matallah M. & Ivorra S. (2021). Sensitivity of spatial variable seismic ground motion to multiple local site conditions. 9th Turkish Conference on Earthquake Engineering (9TCEE), 2-3 june 2021 (pp. 434-441). Istanbul, Turkey.

[14] Sextos, A. Karakostas, C. Lekidis V. & Papadopoulos S. (2015). Multiple support seismic excitation of the Evripos bridge based on free-field and on-structure recordings. *Structure and Infrastructure Engineering*, 11(11). DOI: 10.1080/15732479.2014.977302.

[15] Zerva, A. & Stephenson WR. (2011). Stochastic characteristics of seismic excitations at a non-uniform (rock and soil) site. *Soil Dynamics and Earthquake Engineering*, 31(9), 1261–1284. DOI: 10.1016/j.soildyn.2011.05.006.

[16] Fontara, IK. Titirla, MD. Wuttke, F. Athanatopoulou, AM. Manolis GD. & Sextos AG. (2015). Multiple support excitation of a bridge based on a BEM analysis of the subsoil-structure interaction phenomenon. COMPDYN 2015 and 5th ECCOMAS Thematic Conference on Computational Methods in Structural Dynamics and Earthquake Engineering At: Crete Island, Greece.

[17] Bard, PY. Campillo, M. Chavez-Garcia FJ. & Sanchez-Sesma F. (1988). Mexico earthquake of September 19, 1985 - a theoretical investigation of large- and small-scale amplification effects in the Mexico City valley. *Earthquake Spectra*, 4(3), 609–633. DOI: 10.1193/1.1585493.

[18] Wang, S. & Hao H. (2002). Effects of random variations of soil properties on site amplification of seismic ground motions. *Soil Dynamics and Earthquake Engineering*, 22(7), 551–564. DOI: 10.1016/S0267-7261(02)00038-6.

[19] Bi, K. & Hao H. (2012). Modelling and simulation of spatially varying earthquake ground motions at sites with varying conditions. *Probabilistic Engineering Mechanics*, 29, 92–104. DOI: 10.1016/j.probengmech.2011.09.002.

[20] Zhang, DY. Liu, W. Xie WC. & Pandey MD. (2013). Modeling of spatially correlated, site-reflected, and nonstationary ground motions compatible with response spectrum. *Soil Dynamics and Earthquake Engineering*, 55, 21–32. DOI: 10.1016/j.soildyn.2013.08.002.

[21] Derbal, R. Benmansour N. & Djafour M. (2018). Impact of spatial variability of earthquake ground motion on seismic response of a railway bridge. *International Journal of Computational Methods and Experimental Measurements*, 6(3), 910–920. DOI: 10.2495/cmem-v6-n5-910-920.

[22] Adanur, S. Altunişik, AC. Soyluk, K. Bayraktar A. & Dumanoğlu AA. (2016). Multiple-support seismic response of Bosporus Suspension Bridge for various random vibration methods. *Case Studies in Structural Engineering*, 5, 54–67. DOI: 10.1016/j.csse.2016.04.001.

[23] Li, C. Li, H. Hao, H. Bi K. & Tian L. (2018). Simulation of multi-support depth-varying earthquake ground motions within heterogeneous onshore and offshore sites. *Earthq Eng & Eng Vib*, 17(3), 475–490. DOI: 10.1007/s11803-018-0456-7.

[24] Shiravand, MR. & Parvanehro P. (2019). Spatial variation of seismic ground motion effects on nonlinear responses of cable stayed bridges considering different soil types. *Soil Dynamics and Earthquake Engineering*, 119, 104–117. DOI: 10.1016/j.soildyn.2019.01.002.

[25] Boudina, A. & Hammoutene M. (2020). Generation of seismic excitations compatible with target spectrum: application to Eurocode 8. *World Journal of Engineering*, 18(1), 122–135. DOI: 10.1108/WJE-02-2020-0042.

[26] Liu, G. Liu, Y. Han B. & Lian J. (2020). Theoretical and numerical approach for simulating spatially variable seismic underground motions in layered saturated media. *Journal of Earthquake Engineering*, 24(4), 601–627. DOI: 10.1080/13632469.2018.1452809.

[27] Loyola, L. Rojas F. & Ruiz RO. (2021). Synthetic stochastic ground motions compatible with the Chilean seismic hazard. *Engineering Structures*, 228. DOI: 10.1016/j.engstruct.2020.111471.

[28] Muscolino, G. Genovese, F. Biondi G. & Cascone E. (2021). Generation of fully non-stationary random processes consistent with target seismic accelerograms. *Soil Dynamics and Earthquake Engineering*, 141: 106467. DOI: 10.1016/J.SOILDYN.2020.106467.

[29] Rodda, GK. & Basu D. (2018). Spatial variation and conditional simulation of seismic ground motion. *Bulletin of Earthquake Engineering*, 16(10), 4399–4426. DOI: 10.1007/s10518-018-0397-6.

[30] Rodda, GK. & Basu D. (2020). Spatially correlated vertical ground motion for seismic design. *Engineering Structures*, 206, 110191. DOI: 10.1016/j.engstruct.2020.110191.

[31] Benmansour, N. (2013). *Effet de la variabilité spatiale du mouvement sismique sur le comportement dynamique des ponts*. University of Tlemcen – Aboubakr Belkaid, Tlemcen, Algeria.

[32] Benmansour, N. Djafour, M. Bekkouche, A. Zendagui D. & Benyacoub A. (2012). Seismic response evaluation of bridges under differential ground motion: A comparison with the new Algerian provisions. *European Journal of Environmental and Civil Engineering*, 16(7), 863–881. DOI: 10.1080/19648189.2012.681951.

[33] Wolf, JP. (1985). *Dynamic Soil-Structure Interaction*.

[34] Şafak, E. (1995). Discrete-Time Analysis of Seismic Site Amplification. *Journal of Engineering Mechanics*, 121(7), 801–809. DOI: 10.1061/(asce)0733-9399(1995)121:7(801).

[35] Deodatis, G. (1996). Non-stationary stochastic vector processes: Seismic ground motion applications. *Probabilistic Engineering Mechanics*, 11(3), 149–167. DOI: 10.1016/0266-8920(96)00007-0.

[36] Bi, K. & Hao H. (2012). Influence of ground motion spatial variations and local soil conditions on the seismic responses of buried segmented pipelines. *Structural Engineering and Mechanics*, 44, 663-680. DOI: 10.12989/sem.2012.44.5.663.

[37] Jennings, PC. Housner GW. & Tsai NC. (1968). *Simulated earthquake motions*. A report on research conducted under a grant from the National Science Foundation, Pasadena, California, USA.

[38] Clough, RW. & Penzien J. (1993). *Dynamics of structures*. 2nd edition. New York: mcgraw-Hill.

[39] Tajimi, HA. (1960). Statistical method of determining the maximum response of a building structure during an earthquake. In: Proceedings of the second world conference Engineering E, editor., Tokyo and Kyoto, Japan, 1960.

[40] MTP, (2010). *Règles parasismiques applicables au domaine des ouvrages d'art*. Ministère des Travaux Publics, Alger.

[41] CEN, (2004). *Eurocode 8: Design provisions of structures for earthquake resistance-part1: General rules, Seismic Actions and Rules for buildings*, EN1998-1:2004. Brussels, Belgium.

[42] Li, C. Hao, H. Li, H. Bi K. & Chen B. (2017). Modeling and simulation of spatially correlated ground motions at multiple onshore and offshore sites. *Journal of Earthquake Engineering*, 21(3), 359-383. DOI: 10.1080/13632469.2016.1172375.